Search for the Rare Decay $B^0 \to \tau^+\tau^-$ at *BABAR*

B. Aubert,[1] R. Barate,[1] D. Boutigny,[1] F. Couderc,[1] Y. Karyotakis,[1] J. P. Lees,[1] V. Poireau,[1] V. Tisserand,[1] A. Zghiche,[1] E. Grauges,[2] A. Palano,[3] M. Pappagallo,[3] A. Pompili,[3] J. C. Chen,[4] N. D. Qi,[4] G. Rong,[4] P. Wang,[4] Y. S. Zhu,[4] G. Eigen,[5] I. Ofte,[5] B. Stugu,[5] G. S. Abrams,[6] M. Battaglia,[6] A. B. Breon,[6] D. N. Brown,[6] J. Button-Shafer,[6] R. N. Cahn,[6] E. Charles,[6] C. T. Day,[6] M. S. Gill,[6] A. V. Gritsan,[6] Y. Groysman,[6] R. G. Jacobsen,[6] R. W. Kadel,[6] J. Kadyk,[6] L. T. Kerth,[6] Yu. G. Kolomensky,[6] G. Kukartsev,[6] G. Lynch,[6] L. M. Mir,[6] P. J. Oddone,[6] T. J. Orimoto,[6] M. Pripstein,[6] N. A. Roe,[6] M. T. Ronan,[6] W. A. Wenzel,[6] M. Barrett,[7] K. E. Ford,[7] T. J. Harrison,[7] A. J. Hart,[7] C. M. Hawkes,[7] S. E. Morgan,[7] A. T. Watson,[7] M. Fritsch,[8] K. Goetzen,[8] T. Held,[8] H. Koch,[8] B. Lewandowski,[8] M. Pelizaeus,[8] K. Peters,[8] T. Schroeder,[8] M. Steinke,[8] J. T. Boyd,[9] J. P. Burke,[9] N. Chevalier,[9] W. N. Cottingham,[9] T. Cuhadar-Donszelmann,[10] B. G. Fulsom,[10] C. Hearty,[10] N. S. Knecht,[10] T. S. Mattison,[10] J. A. McKenna,[10] A. Khan,[11] P. Kyberd,[11] M. Saleem,[11] L. Teodorescu,[11] A. E. Blinov,[12] V. E. Blinov,[12] A. D. Bukin,[12] V. P. Druzhinin,[12] V. B. Golubev,[12] E. A. Kravchenko,[12] A. P. Onuchin,[12] S. I. Serednyakov,[12] Yu. I. Skovpen,[12] E. P. Solodov,[12] A. N. Yushkov,[12] D. Best,[13] M. Bondioli,[13] M. Bruinsma,[13] M. Chao,[13] S. Curry,[13] I. Eschrich,[13] D. Kirkby,[13] A. J. Lankford,[13] P. Lund,[13] M. Mandelkern,[13] R. K. Mommsen,[13] W. Roethel,[13] D. P. Stoker,[13] C. Buchanan,[14] B. L. Hartfiel,[14] A. J. R. Weinstein,[14] S. D. Foulkes,[15] J. W. Gary,[15] O. Long,[15] B. C. Shen,[15] K. Wang,[15] L. Zhang,[15] D. del Re,[16] H. K. Hadavand,[16] E. J. Hill,[16] D. B. MacFarlane,[16] H. P. Paar,[16] S. Rahatlou,[16] V. Sharma,[16] J. W. Berryhill,[17] C. Campagnari,[17] A. Cunha,[17] B. Dahmes,[17] T. M. Hong,[17] M. A. Mazur,[17] J. D. Richman,[17] W. Verkerke,[17] T. W. Beck,[18] A. M. Eisner,[18] C. J. Flacco,[18] C. A. Heusch,[18] J. Kroseberg,[18] W. S. Lockman,[18] G. Nesom,[18] T. Schalk,[18] B. A. Schumm,[18] A. Seiden,[18] P. Spradlin,[18] D. C. Williams,[18] M. G. Wilson,[18] J. Albert,[19] E. Chen,[19] G. P. Dubois-Felsmann,[19] A. Dvoretskii,[19] D. G. Hitlin,[19] I. Narsky,[19] T. Piatenko,[19] F. C. Porter,[19] A. Ryd,[19] A. Samuel,[19] R. Andreassen,[20] G. Mancinelli,[20] B. T. Meadows,[20] M. D. Sokoloff,[20] F. Blanc,[21] P. Bloom,[21] S. Chen,[21] W. T. Ford,[21] J. F. Hirschauer,[21] A. Kreisel,[21] U. Nauenberg,[21] A. Olivas,[21] P. Rankin,[21] W. O. Ruddick,[21] J. G. Smith,[21] K. A. Ulmer,[21] S. R. Wagner,[21] J. Zhang,[21] A. Chen,[22] E. A. Eckhart,[22] J. L. Harton,[22] A. Soffer,[22] W. H. Toki,[22] R. J. Wilson,[22] Q. Zeng,[22] R. Aleksan,[23] S. Emery,[23] A. Gaidot,[23] S. F. Ganzhur,[23] P.-F. Giraud,[23] G. Graziani,[23] G. Hamel de Monchenault,[23] W. Kozanecki,[23] M. Legendre,[23] G. W. London,[23] B. Mayer,[23] G. Vasseur,[23] Ch. Yeche,[23] M. Zito,[23] D. Altenburg,[24] E. Feltresi,[24] A. Hauke,[24] B. Spaan,[24] T. Brandt,[25] J. Brose,[25] M. Dickopp,[25] V. Klose,[25] H. M. Lacker,[25] R. Nogowski,[25] S. Otto,[25] A. Petzold,[25] J. Schubert,[25] K. R. Schubert,[25] R. Schwierz,[25] J. E. Sundermann,[25] D. Bernard,[26] G. R. Bonneaud,[26] P. Grenier,[26] S. Schrenk,[26] Ch. Thiebaux,[26] G. Vasileiadis,[26] M. Verderi,[26] D. J. Bard,[27] P. J. Clark,[27] W. Gradl,[27] F. Muheim,[27] S. Playfer,[27] Y. Xie,[27] M. Andreotti,[28] V. Azzolini,[28] D. Bettoni,[28] C. Bozzi,[28] R. Calabrese,[28] G. Cibinetto,[28] E. Luppi,[28] M. Negrini,[28] L. Piemontese,[28] F. Anulli,[29] R. Baldini-Ferroli,[29] A. Calcaterra,[29] R. de Sangro,[29] G. Finocchiaro,[29] P. Patteri,[29] I. M. Peruzzi,[29] M. Piccolo,[29] A. Zallo,[29] A. Buzzo,[30] R. Capra,[30] R. Contri,[30] M. Lo Vetere,[30] M. Macri,[30] M. R. Monge,[30] S. Passaggio,[30] C. Patrignani,[30] E. Robutti,[30] A. Santroni,[30] S. Tosi,[30] G. Brandenburg,[31] K. S. Chaisanguanthum,[31] M. Morii,[31] E. Won,[31] J. Wu,[31] R. S. Dubitzky,[32] U. Langenegger,[32] J. Marks,[32] S. Schenk,[32] U. Uwer,[32] F. Martinez-Vidal,[33] W. Bhimji,[34] D. A. Bowerman,[34] P. D. Dauncey,[34] U. Egede,[34] R. L. Flack,[34] J. R. Gaillard,[34] G. W. Morton,[34] J. A. Nash,[34] M. B. Nikolich,[34] G. P. Taylor,[34] W. P. Vazquez,[34] M. J. Charles,[35] W. F. Mader,[35] U. Mallik,[35] A. K. Mohapatra,[35] J. Cochran,[36] H. B. Crawley,[36] V. Eyges,[36] W. T. Meyer,[36] S. Prell,[36] E. I. Rosenberg,[36] A. E. Rubin,[36] J. Yi,[36] M. Biasini,[37] R. Covarelli,[37] S. Pacetti,[37] M. Pioppi,[37] N. Arnaud,[38] M. Davier,[38] X. Giroux,[38] G. Grosdidier,[38] A. Höcker,[38] F. Le Diberder,[38] V. Lepeltier,[38] A. M. Lutz,[38] A. Oyanguren,[38] T. C. Petersen,[38] M. Pierini,[38] S. Plaszczynski,[38] S. Rodier,[38] P. Roudeau,[38] M. H. Schune,[38] A. Stocchi,[38] G. Wormser,[38] C. H. Cheng,[39] D. J. Lange,[39] M. C. Simani,[39] D. M. Wright,[39] A. J. Bevan,[40] C. A. Chavez,[40] Ian J. Forster,[40] J. R. Fry,[40] E. Gabathuler,[40] R. Gamet,[40] K. A. George,[40] D. E. Hutchcroft,[40] R. J. Parry,[40] D. J. Payne,[40] K. C. Schofield,[40] C. Touramanis,[40] C. M. Cormack,[41] F. Di Lodovico,[41] W. Menges,[41] R. Sacco,[41] C. L. Brown,[42] G. Cowan,[42] H. U. Flaecher,[42] M. G. Green,[42] D. A. Hopkins,[42] P. S. Jackson,[42] T. R. McMahon,[42] S. Ricciardi,[42] F. Salvatore,[42] D. Brown,[43] C. L. Davis,[43] J. Allison,[44] N. R. Barlow,[44] R. J. Barlow,[44] C. L. Edgar,[44] M. C. Hodgkinson,[44] M. P. Kelly,[44] G. D. Lafferty,[44] M. T. Naisbit,[44] J. C. Williams,[44] C. Chen,[45] W. D. Hulsbergen,[45] A. Jawahery,[45] D. Kovalskyi,[45] C. K. Lae,[45] D. A. Roberts,[45] G. Simi,[45] G. Blaylock,[46] C. Dallapiccola,[46] S. S. Hertzbach,[46] R. Kofler,[46] V. B. Koptchev,[46] X. Li,[46] T. B. Moore,[46] S. Saremi,[46] H. Staengle,[46] S. Willocq,[46] R. Cowan,[47] K. Koeneke,[47] G. Sciolla,[47] S. J. Sekula,[47] M. Spitznagel,[47] F. Taylor,[47] R. K. Yamamoto,[47] H. Kim,[48] P. M. Patel,[48] S. H. Robertson,[48] A. Lazzaro,[49] V. Lombardo,[49] F. Palombo,[49] J. M. Bauer,[50] L. Cremaldi,[50] V. Eschenburg,[50] R. Godang,[50] R. Kroeger,[50] J. Reidy,[50] D. A. Sanders,[50] D. J. Summers,[50] H. W. Zhao,[50] S. Brunet,[51]

D. Cote,[51] P. Taras,[51] B. Viaud,[51] H. Nicholson,[52] M. Baak,[53] H. Bulten,[53] G. Raven,[53] H. L. Snoek,[53] L. Wilden,[53] N. Cavallo,[54] G. De Nardo,[54] F. Fabozzi,[54] C. Gatto,[54] L. Lista,[54] D. Monorchio,[54] P. Paolucci,[54] D. Piccolo,[54] C. Sciacca,[54] C. P. Jessop,[55] J. M. LoSecco,[55] T. Allmendinger,[56] G. Benelli,[56] K. K. Gan,[56] K. Honscheid,[56] D. Hufnagel,[56] P. D. Jackson,[56] H. Kagan,[56] R. Kass,[56] T. Pulliam,[56] A. M. Rahimi,[56] R. Ter-Antonyan,[56] Q. K. Wong,[56] J. Brau,[57] R. Frey,[57] O. Igonkina,[57] M. Lu,[57] C. T. Potter,[57] N. B. Sinev,[57] D. Strom,[57] J. Strube,[57] E. Torrence,[57] F. Galeazzi,[58] M. Margoni,[58] M. Morandin,[58] M. Posocco,[58] M. Rotondo,[58] F. Simonetto,[58] R. Stroili,[58] C. Voci,[58] M. Benayoun,[59] H. Briand,[59] J. Chauveau,[59] P. David,[59] C. de la Vaissiere,[59] L. Del Buono,[59] O. Hamon,[59] M. J. J. John,[59] Ph. Leruste,[59] J. Malcles,[59] J. Ocariz,[59] L. Roos,[59] G. Therin,[59] P. K. Behera,[60] L. Gladney,[60] Q. H. Guo,[60] J. Panetta,[60] C. Angelini,[61] G. Batignani,[61] S. Bettarini,[61] F. Bucci,[61] G. Calderini,[61] M. Carpinelli,[61] R. Cenci,[61] F. Forti,[61] M. A. Giorgi,[61] A. Lusiani,[61] G. Marchiori,[61] M. Morganit,[61] N. Neri,[61] E. Paoloni,[61] M. Rama,[61] G. Rizzo,[61] J. Walsh,[61] M. Haire,[62] D. Judd,[62] D. E. Wagoner,[62] J. Biesiada,[63] N. Danielson,[63] P. Elmer,[63] Y. Lau,[63] C. Lu,[63] J. Olsen,[63] A. J. S. Smith,[63] A. V. Telnov,[63] F. Bellini,[64] G. Cavoto,[64] A. D'Orazio,[64] E. Di Marco,[64] R. Faccini,[64,*] F. Ferrarotto,[64] F. Ferroni,[64] M. Gaspero,[64] L. Li Gioi,[64] M. A. Mazzoni,[64] S. Morganti,[64] G. Piredda,[64] F. Polci,[64] F. Safai Tehrani,[64] C. Voena,[64] H. Schröder,[65] G. Wagner,[65] R. Waldi,[65] T. Adye,[66] N. De Groot,[66] B. Franek,[66] G. P. Gopal,[66] E. O. Olaiya,[66] F. F. Wilson,[66] M. V. Purohit,[67] A. W. Weidemann,[67] J. R. Wilson,[67] F. X. Yumiceva,[67] T. Abe,[68] M. T. Allen,[68] D. Aston,[68] R. Bartoldus,[68] N. Berger,[68] A. M. Boyarski,[68] O. L. Buchmueller,[68] R. Claus,[68] J. P. Coleman,[68] M. R. Convery,[68] M. Cristinziani,[68] J. C. Dingfelder,[68] D. Dong,[68] J. Dorfan,[68] D. Dujmic,[68] W. Dunwoodie,[68] S. Fan,[68] R. C. Field,[68] T. Glanzman,[68] S. J. Gowdy,[68] T. Hadig,[68] V. Halyo,[68] C. Hast,[68] T. Hryn'ova,[68] W. R. Innes,[68] M. H. Kelsey,[68] P. Kim,[68] M. L. Kocian,[68] D. W. G. S. Leith,[68] J. Libby,[68] S. Luitz,[68] V. Luth,[68] H. L. Lynch,[68] H. Marsiske,[68] R. Messner,[68] D. R. Muller,[68] C. P. O'Grady,[68] V. E. Ozcan,[68] A. Perazzo,[68] M. Perl,[68] B. N. Ratcliff,[68] A. Roodman,[68] A. A. Salnikov,[68] R. H. Schindler,[68] J. Schwiening,[68] A. Snyder,[68] J. Stelzer,[68] D. Su,[68] M. K. Sullivan,[68] K. Suzuki,[68] S. K. Swain,[68] J. M. Thompson,[68] J. Va'vra,[68] N. van Bakel,[68] M. Weaver,[68] W. J. Wisniewski,[68] M. Wittgen,[68] D. H. Wright,[68] A. K. Yarritu,[68] K. Yi,[68] C. C. Young,[68] P. R. Burchat,[69] A. J. Edwards,[69] S. A. Majewski,[69] B. A. Petersen,[69] C. Roat,[69] M. Ahmed,[70] S. Ahmed,[70] M. S. Alam,[70] R. Bula,[70] J. A. Ernst,[70] M. A. Saeed,[70] F. R. Wappler,[70] S. B. Zain,[70] W. Bugg,[71] M. Krishnamurthy,[71] S. M. Spanier,[71] R. Eckmann,[72] J. L. Ritchie,[72] A. Satpathy,[72] R. F. Schwitters,[72] J. M. Izen,[73] I. Kitayama,[73] X. C. Lou,[73] S. Ye,[73] F. Bianchi,[74] M. Bona,[74] F. Gallo,[74] D. Gamba,[74] M. Bomben,[75] L. Bosisio,[75] C. Cartaro,[75] F. Cossutti,[75] G. Della Ricca,[75] S. Dittongo,[75] S. Grancagnolo,[75] L. Lanceri,[75] L. Vitale,[75] R. S. Panvini,[76] Sw. Banerjee,[77] B. Bhuyan,[77] C. M. Brown,[77] D. Fortin,[77] K. Hamano,[77] R. Kowalewski,[77] J. M. Roney,[77] R. J. Sobie,[77] J. J. Back,[78] P. F. Harrison,[78] T. E. Latham,[78] G. B. Mohanty,[78] H. R. Band,[79] X. Chen,[79] B. Cheng,[79] S. Dasu,[79] M. Datta,[79] A. M. Eichenbaum,[79] K. T. Flood,[79] M. Graham,[79] J. J. Hollar,[79] J. R. Johnson,[79] P. E. Kutter,[79] H. Li,[79] R. Liu,[79] B. Mellado,[79] A. Mihalyi,[79] Y. Pan,[79] R. Prepost,[79] P. Tan,[79] J. H. von Wimmersperg-Toeller,[79] S. L. Wu,[79] Z. Yu,[79] H. Neal,[80] and G. Schott[81]

(*BABAR* Collaboration)

[1]*Laboratoire de Physique des Particules, F-74941 Annecy-le-Vieux, France*
[2]*Facultat de Fisica ECM, Universitat de Barcelona, E-08028 Barcelona, Spain*
[3]*Dipartimento di Fisica and INFN, Università di Bari, I-70126 Bari, Italy*
[4]*Institute of High Energy Physics, Beijing 100039, China*
[5]*Institute of Physics, University of Bergen, N-5007 Bergen, Norway*
[6]*Lawrence Berkeley National Laboratory, Berkeley, California 94720, USA, and University of California at Berkeley, Berkeley, California 94720, USA*
[7]*University of Birmingham, Birmingham B15 2TT, United Kingdom*
[8]*Institut für Experimentalphysik 1, Ruhr Universität Bochum, D-44780 Bochum, Germany*
[9]*University of Bristol, Bristol BS8 1TL, United Kingdom*
[10]*University of British Columbia, Vancouver, British Columbia V6T 1Z1, Canada*
[11]*Brunel University, Uxbridge, Middlesex UB8 3PH, United Kingdom*
[12]*Budker Institute of Nuclear Physics, Novosibirsk 630090, Russia*
[13]*University of California at Irvine, Irvine, California 92697, USA*
[14]*University of California at Los Angeles, Los Angeles, California 90024, USA*
[15]*University of California at Riverside, Riverside, California 92521, USA*
[16]*University of California at San Diego, La Jolla, California 92093, USA*
[17]*University of California at Santa Barbara, Santa Barbara, California 93106, USA*
[18]*Institute for Particle Physics, University of California at Santa Cruz, Santa Cruz, California 95064, USA*

[19]California Institute of Technology, Pasadena, California 91125, USA
[20]University of Cincinnati, Cincinnati, Ohio 45221, USA
[21]University of Colorado, Boulder, Colorado 80309, USA
[22]Colorado State University, Fort Collins, Colorado 80523, USA
[23]DSM/Dapnia, CEA/Saclay, F-91191 Gif-sur-Yvette, France
[24]Institut für Physik, Universität Dortmund, D-44221 Dortmund, Germany
[25]Institut für Kern- und Teilchenphysik, Technische Universität Dresden, D-01062 Dresden, Germany
[26]Ecole Polytechnique, LLR, F-91128 Palaiseau, France
[27]University of Edinburgh, Edinburgh EH9 3JZ, United Kingdom
[28]Dipartimento di Fisica and INFN, Università di Ferrara, I-44100 Ferrara, Italy
[29]Laboratori Nazionali di Frascati dell'INFN, I-00044 Frascati, Italy
[30]Dipartimento di Fisica and INFN, Università di Genova, I-16146 Genova, Italy
[31]Harvard University, Cambridge, Massachusetts 02138, USA
[32]Universität Heidelberg, Philosophenweg 12, D-69120 Heidelberg, Germany
[33]IFIC, Universitat de Valencia-CSIC, E-46071 Valencia, Spain
[34]Imperial College London, London SW7 2AZ, United Kingdom
[35]University of Iowa, Iowa City, Iowa 52242, USA
[36]Iowa State University, Ames, Iowa 50011-3160, USA
[37]Instituto Nazionale di Fisica Nucleare, I-06100 Perugia, Italy
[38]Laboratoire de l'Accélérateur Linéaire, F-91898 Orsay, France
[39]Lawrence Livermore National Laboratory, Livermore, California 94550, USA
[40]University of Liverpool, Liverpool L69 72E, United Kingdom
[41]Queen Mary, University of London, London E1 4NS, United Kingdom
[42]University of London, Royal Holloway and Bedford New College, Egham, Surrey TW20 0EX, United Kingdom
[43]University of Louisville, Louisville, Kentucky 40292, USA
[44]University of Manchester, Manchester M13 9PL, United Kingdom
[45]University of Maryland, College Park, Maryland 20742, USA
[46]University of Massachusetts, Amherst, Massachusetts 01003, USA
[47]Laboratory for Nuclear Science, Massachusetts Institute of Technology, Cambridge, Massachusetts 02139, USA
[48]McGill University, Montréal, Quebec H3A 2T8, Canada
[49]Dipartimento di Fisica and INFN, Università di Milano, I-20133 Milano, Italy
[50]University of Mississippi, University, Mississippi 38677, USA
[51]Laboratoire René J. A. Lévesque, Université de Montréal, Montréal, Quebec H3C 3J7, Canada
[52]Mount Holyoke College, South Hadley, Massachusetts 01075, USA
[53]NIKHEF, National Institute for Nuclear Physics and High Energy Physics, NL-1009 DB Amsterdam, The Netherlands
[54]Dipartimento di Scienze Fisiche and INFN, Università di Napoli Federico II, I-80126 Napoli, Italy
[55]University of Notre Dame, Notre Dame, Indiana 46556, USA
[56]The Ohio State University, Columbus, Ohio 43210, USA
[57]University of Oregon, Eugene, Oregon 97403, USA
[58]Dipartimento di Fisica and INFN, Università di Padova, I-35131 Padova, Italy
[59]Laboratoire de Physique Nucléaire H. E., Universités Paris VI et VII, F-75252 Paris, France
[60]University of Pennsylvania, Philadelphia, Pennsylvania 19104, USA
[61]Dipartimento di Fisica, Scuola Normale Superiore and INFN, Università di Pisa, I-56127 Pisa, Italy
[62]Prairie View A&M University, Prairie View, Texas 77446, USA
[63]Princeton University, Princeton, New Jersey 08544, USA
[64]Dipartimento di Fisica and INFN, Università di Roma La Sapienza, I-00185 Roma, Italy
[65]Universität Rostock, D-18051 Rostock, Germany
[66]Rutherford Appleton Laboratory, Chilton, Didcot, Oxon OX11 0QX, United Kingdom
[67]University of South Carolina, Columbia, South Carolina 29208, USA
[68]Stanford Linear Accelerator Center, Stanford, California 94309, USA
[69]Stanford University, Stanford, California 94305-4060, USA
[70]State University of New York, Albany, New York 12222, USA
[71]University of Tennessee, Knoxville, Tennessee 37996, USA
[72]University of Texas at Austin, Austin, Texas 78712, USA
[73]University of Texas at Dallas, Richardson, Texas 75083, USA
[74]Dipartimento di Fisica Sperimentale and INFN, Università di Torino, I-10125 Torino, Italy
[75]Dipartimento di Fisica and INFN, Università di Trieste, I-34127 Trieste, Italy
[76]Vanderbilt University, Nashville, Tennessee 37235, USA
[77]University of Victoria, Victoria, British Columbia V8W 3P6, Canada
[78]University of Warwick, Coventry, Warwicks CV4 7AL, United Kingdom
[79]University of Wisconsin, Madison, Wisconsin 53706, USA

[80]Yale University, New Haven, Connecticut 06511, USA
[81]Institut für Experimentelle Kernphysik (IEKP), University of Karlsruhe, Postfach 3640, D-76021 Karlsruhe, Germany
(Received 9 November 2005; published 23 June 2006)

We present the results of a search for the decay $B^0 \to \tau^+\tau^-$ in a data sample of $(232 \pm 3) \times 10^6$ $\Upsilon(4S) \to B\bar{B}$ decays using the *BABAR* detector. Certain extensions of the standard model predict measurable levels of this otherwise rare decay. We reconstruct fully one neutral B meson and seek evidence for the signal decay in the rest of the event. We find no evidence for signal events and obtain $\mathcal{B}(B^0 \to \tau^+\tau^-) < 4.1 \times 10^{-3}$ at the 90% confidence level.

DOI: 10.1103/PhysRevLett.96.241802 PACS numbers: 13.20.He, 14.40.Nd, 14.60.Fg

None of the leptonic decays $B^0 \to \ell^+\ell^-$ ($\ell = e, \mu, \tau$) have been observed. In the standard model of particle physics, the decays can be mediated by box and penguin diagrams (Fig. 1). The standard model produces only the combinations $\ell_R^+\ell_L^-$ and $\ell_L^+\ell_R^-$. The amplitudes for the decay of a spin-zero particle to these states are proportional to m_ℓ and thus the decay rates are suppressed by $(m_\ell/m_B)^2$. The suppression is smallest for $B^0 \to \tau^+\tau^-$ due to the large τ mass. The standard model prediction for the $B^0 \to \tau^+\tau^-$ branching fraction is [1]

$$\mathcal{B}^{\mathrm{SM}}(B^0 \to \tau^+\tau^-) = 1.2 \times 10^{-7}\left[\frac{f_B}{200\ \mathrm{MeV}}\right]^2\left[\frac{|V_{td}|}{0.007}\right]^2, \quad (1)$$

where f_B is the B decay constant and V_{td} is the Cabibbo-Kobayashi-Maskawa matrix element. The theoretical uncertainty on f_B and the experimental error on V_{td} dominate the uncertainty on the predicted branching fraction.

Extensions of the standard model containing leptoquarks, which couple leptons to quarks, predict enhancements for $\mathcal{B}(B^0 \to \tau^+\tau^-)$ [2] that are proportional to the square of the leptoquark coupling. In theories that contain two Higgs doublet fields, the rate can be enhanced by powers of $\tan\beta$, the ratio of vacuum expectation values of the two Higgs doublet fields [3,4]. Since $B^0 \to \ell^+\ell^-$ has not been observed, one can only constrain model parameters using the measured branching fraction limits. While $\tan\beta$ is constrained by all three modes ($\ell = e, \mu, \tau$), only $B^0 \to \tau^+\tau^-$ can constrain the coupling of a leptoquark to the third lepton generation or other new physics involving only the third generation.

The analysis described here provides the first upper limit on $\mathcal{B}(B^0 \to \tau^+\tau^-)$. The data were collected with the *BABAR* detector at the asymmetric PEP-II e^+e^- storage ring. A full description of the *BABAR* detector is given in Ref. [5]. In brief, charged-particle momenta are measured with a tracking system comprised of a silicon vertex detector (SVT) and a drift chamber (DCH) placed within a highly uniform 1.5-T magnetic field generated by a superconducting solenoid. Electron and photon energies are measured with an electromagnetic calorimeter (EMC) constructed with thalium-doped CsI scintillating crystals. Muons are distinguished from hadrons in a steel magnetic-flux return instrumented with resistive plate chambers (IFR). Charged-particle identification is provided by a Cherenkov detector (DIRC) and the tracking system. The data sample consists of 210 fb^{-1} collected at the peak of the $\Upsilon(4S)$ resonance, which corresponds to $232 \pm 3 \times 10^6$ $B\bar{B}$ pairs. The expected background and the expected signal efficiency are obtained from Monte Carlo simulation samples. The sample events were generated with the EVTGEN event simulator [6] and propagated through a detailed model of the *BABAR* detector using the GEANT4 detector simulator [7].

Isolating $B^0 \to \tau^+\tau^-$ poses a unique challenge. This decay contains at least two and as many as four neutrinos, so there is no kinematic discriminant that separates signal from background due to undetected particles. Since two B mesons are produced in an $\Upsilon(4S)$ decay, the misassignment of decay products to the parent B must be avoided. We completely reconstruct one B candidate in each event (hereafter referred to as the companion B) and search for the signal decay among the remaining detected particles. The combinatorial background in the companion-B reconstruction is determined by a fit to the companion-B invariant mass distribution. We employ the parameters

$$m_{\mathrm{ES}} = \sqrt{E^{*2}_{\mathrm{beam}} - p^{*2}_B}, \quad (2)$$

$$\Delta E = E^*_B - E^*_{\mathrm{beam}}, \quad (3)$$

where p^*_B and E^*_B are the reconstructed companion-B momentum and energy in the center-of-mass (c.m.) frame. E^*_{beam} is the beam energy in the c.m. frame. The m_{ES} distributions are fit with a probability density function composed of a Crystal Ball function [8] to model the

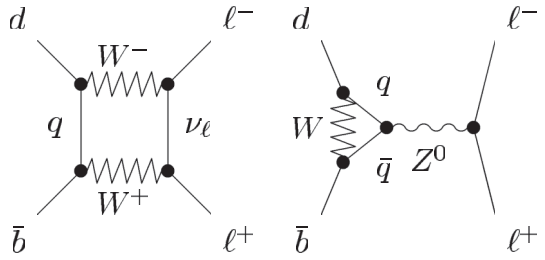

FIG. 1. Standard model box and penguin processes that can mediate $B^0 \to \ell^+\ell^-$ ($q = t, c, u$).

peak at the B mass and an ARGUS function [9] to model the nonpeaking combinatorial background.

The companion B is fully reconstructed in a hadronic mode $\bar{B}^0 \to D^{(*)}X$, where $D^{(*)}$ is either a D^+ [10], D^0, or D^{*+} and X is a system consisting of up to five particles of the type $\pi^\pm$, π^0, $K^\pm$, or K^0_S [11]. D^{*+} mesons are reconstructed in the channel $D^0\pi^+$. D^0 mesons are reconstructed in the channels $K^-\pi^+$, $K^-\pi^+\pi^0$, $K^-\pi^+\pi^-\pi^+$, and $K^0_S\pi^+\pi^-$. D^+ mesons are reconstructed in the channels $K^0_S\pi^+$, $K^-\pi^+\pi^+$, $K^0_S\pi^+\pi^0$, $K^0_S\pi^+\pi^+\pi^-$, and $K^+K^-\pi^+$. The ΔE of the companion B is required to be within two mode-dependent standard deviations of the mean when no π^0 is present, or to satisfy $-0.09 < \Delta E < 0.06$ GeV for reconstructions with one or more π^0. If more than one B candidate is reconstructed in the same mode, the reconstructed B with the smallest $|\Delta E|$ is selected. For each mode, the purity $B_{\rm pur}$ is the ratio of the number of events before signal selection in the fitted peak to the total number of events in the region $5.27 < m_{\rm ES} < 5.29$ GeV. Only events reconstructed in a mode with $B_{\rm pur} > 0.12$ are selected, which results in the reconstruction of 147 distinct modes in the data sample. If B candidates are reconstructed in more than one mode, the B reconstructed in the mode with the highest $B_{\rm pur}$ is selected as the companion B.

We estimate the total companion-B yield from all reconstructed modes using the $B\bar{B}$ and $q\bar{q}$ ($q = u, d, s, c$) simulated samples before applying the signal $B^0 \to \tau^+\tau^-$ selection. We first remove the peak from the $B^0\bar{B}^0$ simulated sample using the fitted Crystal Ball probability density function. Subtracting the simulated combinatorial background $m_{\rm ES}$ shape, fitted to the data below 5.26 GeV, from the data distribution yields a nominal companion-B yield of $N_{B^0\bar{B}^0} = (2.80 \pm 0.27) \times 10^5$ (Fig. 2). The systematic error on $N_{B^0\bar{B}^0}$ is estimated to be 10% by varying the fit region and by varying the combinatorial background composition with event-shape-variable cuts.

The companion-B decay products are removed from the event, and the signal-B characteristics are sought among the remaining particles. The dominant background to $B^0 \to \tau^+\tau^-$ arises from decays $b \to W^- c(\to W^+ s)$, in which the s quark hadronizes into a K^0_L that escapes detection and the virtual W^+ and W^- mimic the virtual W^+ and W^- emitted by the signal τ. A secondary background originates in events in which two oppositely charged particles are lost outside the detector fiducial region. We select signal events that are consistent with each τ decaying to a single charged particle (and one or two ν) by selecting events with zero net charge and two tracks in the recoil system. Each track must leave at least 12 hits in the DCH, originate within 10 cm of the beam spot in the beam direction and within 1.5 cm in the transverse direction, and have a transverse momentum of at least 0.1 GeV. To eliminate background originating from $b \to W^- c(\to W^+ s)$ events, the selection rejects events with identified K^+, K^0_S, or K^0_L. The $K^\pm$ candidates are identified

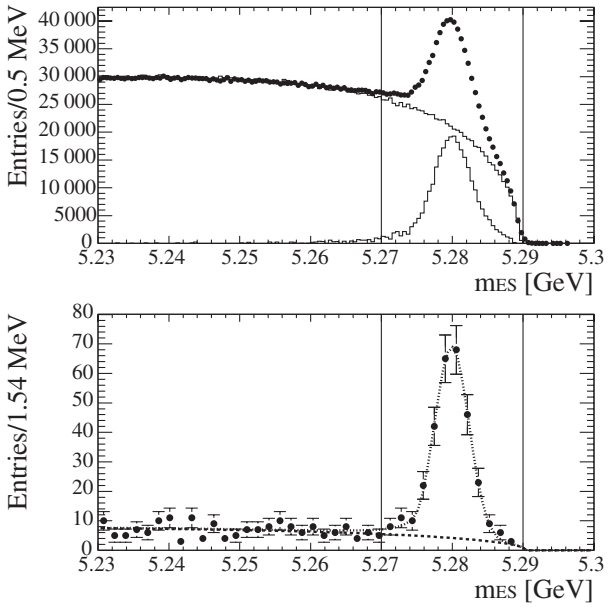

FIG. 2. Top panel: the $m_{\rm ES}$ distribution for the hadronic companion B in data (dots) and scaled simulated background (upper histogram) before the signal $B^0 \to \tau^+\tau^-$ selection is applied; the lower histogram is obtained by subtracting the background from the data. The companion-B yield is $N_{B^0\bar{B}^0} = (2.80 \pm 0.27) \times 10^5$. Bottom panel: the $m_{\rm ES}$ distribution after the signal $B^0 \to \tau^+\tau^-$ selection. The fitted probability density function (short-dashed line) and its ARGUS component (dashed line) are superimposed on the data (dots). We obtain $N_{\rm obs} = 263 \pm 19$ events in the peak.

by a neural network with inputs taken from the SVT, the DCH, and the DIRC. The K^0_S candidates are identified as a $\pi^+\pi^-$ pair with invariant mass consistent with the K^0_S mass ($0.473 < m_{\pi^+\pi^-} < 0.523$ GeV). The K^0_L candidates are identified from clusters in the EMC that have not been associated with a charged track or included in a candidate π^0. A neural network is employed to identify K^0_L candidates using the cluster energy and shower-shape variables, which discriminate hadronic from electromagnetic showers.

The multiplicities of e, μ, and π^0 in the recoil system must be consistent with each τ decaying in one of the channels $\tau \to \pi\nu$, $\rho\nu$, $e\nu\bar{\nu}$, or $\mu\nu\bar{\nu}$ (Table I). The e

TABLE I. Signal $B^0 \to \tau^+\tau^-$ branching fraction and requirements by mode ($\ell = e, \mu$).

Selection mode	$\mathcal{B}$(%) [12]	$N_e + N_\mu$	N_{π^0}	$m_{\pi\pi^0}$
$\tau^+\tau^- \to \ell\nu\bar{\nu}/\ell'\nu\bar{\nu}$	12.4	2	0	
$\tau^+\tau^- \to \ell\nu\bar{\nu}/\pi\nu$	7.8	1	0	
$\tau^+\tau^- \to \ell\nu\bar{\nu}/\rho\nu$	17.7	1	1	[0.6, 1.0] GeV
$\tau^+\tau^- \to \pi\nu/\pi\nu$	1.2	0	0	
$\tau^+\tau^- \to \pi\nu/\rho\nu$	5.6	0	1	[0.6, 1.0] GeV
$\tau^+\tau^- \to \rho\nu/\rho\nu$	6.3	0	2	[0.6, 1.0] GeV

candidates are identified with dE/dx measurements from the DCH and shower-shape variables from the EMC. The μ candidates are identified with variables from the IFR (to reject the π hypothesis) and EMC (to reject the e hypothesis). Track candidates that are not identified as e, μ, or K are assumed to be π. Events with π^0 are vetoed unless the π^0 can be associated with a π^+ such that the invariant mass is consistent with the ρ mass ($0.6 < m_{\pi^+\pi^0} < 1.0$ GeV). The π^0 candidates are formed from pairs of γ candidates with invariant mass $0.090 < m_{\gamma\gamma} < 0.170$ GeV, with each γ having an energy greater than 0.030 GeV. Since the presence of residual unassociated energy in the EMC ($E_{\rm res}$) is a strong indication that an unreconstructed π^0 or K^0 is present, we require $E_{\rm res} < 0.11$ GeV.

The τ-daughter candidates are Lorentz boosted with the companion-B momentum. While distributions of the momenta $\mathbf{p}_+$ and $\mathbf{p}_-$ of the charged daughters exhibit no discrimination from the background momentum distributions, correlations among $|\mathbf{p}_+|$, $|\mathbf{p}_-|$, and $\cos\theta \equiv \mathbf{p}_+ \cdot \mathbf{p}_-/|\mathbf{p}_+||\mathbf{p}_-|$ afford some discrimination, especially when categorized by signal $B^0 \to \tau^+\tau^-$ selection mode. Cascade decay background events manifest an asymmetry in $|\mathbf{p}_+|$ and $|\mathbf{p}_-|$ that is not present in signal events. The parameters $|\mathbf{p}_+|$, $|\mathbf{p}_-|$, $\cos\theta$, $E_{\rm res}$, and the selection mode are used as inputs in a neural-network analysis trained to discriminate signal from background. The final selection requirement is a neural-network output (NN) consistent with signal events.

The signal $B^0 \to \tau^+\tau^-$ selection criteria for $E_{\rm res}$, NN, and $B_{\rm pur}$ are chosen to minimize the expected upper limit on $\mathcal{B}(B^0 \to \tau^+\tau^-)$. That optimization also rejects the signal selection modes $\tau^+\tau^- \to \ell\nu\bar{\nu}/\rho\nu$ and $\tau^+\tau^- \to \pi\nu/\rho\nu$. After the full signal $B^0 \to \tau^+\tau^-$ selection, the combinatorial companion-B background is estimated and subtracted using ARGUS and Crystal Ball fits to the $m_{\rm ES}$ distributions in simulation samples and data (Fig. 2). From these fits we determine the signal efficiency ($\epsilon_{\rm sig}$), the expected number of background events ($N_{\rm expected}$), and the number of observed data events ($N_{\rm obs}$). Including systematic uncertainties described below, we obtain $\epsilon_{\rm sig} = 0.043 \pm 0.009$, and $N_{\rm expected} = 281 \pm 48$. We extract from the fit $N_{\rm obs} = 263 \pm 19$ events in the data after the full selection. The central value of the $B^0 \to \tau^+\tau^-$ branching fraction is $(-1.5 \pm 4.4) \times 10^{-3}$. We find no evidence for signal events. Table II shows $\epsilon_{\rm sig}$, $N_{\rm expected}$, and $N_{\rm obs}$ obtained from individual fits to specific signal selection modes.

Systematic uncertainties on $N_{\rm expected}$ and $\epsilon_{\rm sig}$ arise from several sources. The simulation statistical uncertainty for $N_{\rm expected}$ ($\epsilon_{\rm sig}$) is 10 events (11%). The systematic uncertainties are estimated for cluster corrections to be 8 (3%), for particle identification corrections 10 (10%), and for tracking corrections 7 (3%). The $m_{\rm ES}$ background subtraction fits after the full selection adds a further systematic uncertainty of 4 (2%). We estimate the systematic uncertainty on $N_{\rm expected}$ due to B decay modeling in EVTGEN to be 10%. We estimate the systematic uncertainty due to our model of τ decay by inserting distributions obtained from the specialized τ Monte Carlo code TAUOLA [13] to decay two τ produced with the same helicity and the requisite momentum for a $B^0 \to \tau^+\tau^-$ decay. For each simulated event, the decay mode of each τ is identified and the $|\mathbf{p}_+|$, $|\mathbf{p}_-|$, and $\cos\theta$ values are replaced with values sampled from distributions generated by TAUOLA for that mode. The relative $\epsilon_{\rm sig}$ variation between EVTGEN and TAUOLA simulation is 2%.

TABLE II. $\epsilon_{\rm sig}$, $N_{\rm expected}$, and $N_{\rm obs}$ obtained from individual fits by signal mode. The errors are statistical and fit error added in quadrature. Branching fractions are included in the efficiency estimates. The $\pi\nu/\pi\nu$ channel is dominated by cross feed from other signal channels.

Selection mode	$\epsilon_{\rm sig}$(%)	$N_{\rm expected}$	$N_{\rm obs}$
$\tau^+\tau^- \to \ell\nu\bar{\nu}/\ell'\nu\bar{\nu}$	0.9 ± 0.2	46 ± 4	54 ± 7
$\tau^+\tau^- \to \ell\nu\bar{\nu}/\pi\nu$	1.5 ± 0.3	122 ± 6	105 ± 11
$\tau^+\tau^- \to \pi\nu/\pi\nu$	1.5 ± 0.3	89 ± 6	80 ± 11
$\tau^+\tau^- \to \rho\nu/\rho\nu$	0.3 ± 0.1	21 ± 3	15 ± 6

A final systematic uncertainty for both signal and background is assigned to the modeling of $E_{\rm res}$. The simulation of background hits and hadronic interactions in the EMC does not perfectly model the data, and the discrepancy manifests itself in the $E_{\rm res}$ distribution (Fig. 3). This uncertainty is estimated from the difference between data and the simulation for a control process. The control sample selection is identical to the $B^0 \to \tau^+\tau^-$ selection except that events with an additional reconstructed K^0_S are selected and the K^0_S daughters are removed from the event. For correct K^0_S reconstructions, this control sample models the K^0_L background, while for K^0_S reconstructions from

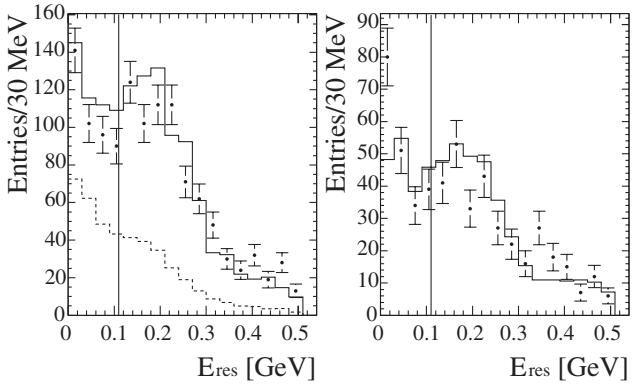

FIG. 3. The $E_{\rm res}$ distribution in the nominal sample (left panel) and the control sample (right panel) for data (dots), simulated background (solid histogram), and simulated signal (dashed histogram). The simulated signal distribution normalization is arbitrary. All requirements except those for $E_{\rm res}$ and NN are imposed. The events to the left of the vertical line are selected.

random combinations of tracks, it models the backgrounds in which two oppositely charged particles are lost due to the limited detector acceptance in the direction of the higher energy beam. The composition of the background in the simulated control sample agrees well with that of the simulated signal sample. The control sample yields are 135 ± 14 events (data) and 125 ± 7 (simulation), for a relative discrepancy of $(8 \pm 13)\%$, consistent with zero. The systematic uncertainty due to modeling the residual energy in the EMC is taken to be the uncertainties in data and simulation yields added in quadrature, namely, 13%.

Systematic uncertainties on the companion-B yield, expected background, and $\epsilon_{\rm sig}$ are folded into the upper limit calculation using the technique described in Ref. [14], giving

$$\mathcal{B}(B^0 \to \tau^+\tau^-) < 4.1 \times 10^{-3}, \tag{4}$$

at the 90% confidence level. The result constrains leptoquark couplings as described in Ref. [2]. For example, the scalar $SU(2)$ doublet leptoquark $S_{1/2}$ can mediate $B^0 \to \tau^+\tau^-$. If no other leptoquark mediates the decay, the product of its coupling λ_R^{33} (coupling right-handed b with τ) with λ_R^{13} (coupling right-handed d with τ) is

$$\lambda_R^{33}\lambda_R^{13} < 1.4 \times 10^{-2}\left[\frac{m_{S_{1/2}}}{100\ \text{GeV}}\right]^2, \tag{5}$$

at the 90% confidence level, where $m_{S_{1/2}}$ is the $S_{1/2}$ mass.

We are grateful for the excellent luminosity and machine conditions provided by our PEP-II colleagues, and for the substantial dedicated effort from the computing organizations that support *BABAR*. The collaborating institutions wish to thank SLAC for its support and kind hospitality. This work is supported by DOE and NSF (USA), NSERC (Canada), IHEP (China), CEA and CNRS-IN2P3 (France), BMBF and DFG (Germany), INFN (Italy), FOM (The Netherlands), NFR (Norway), MIST (Russia), and PPARC (United Kingdom). Individuals have received support from CONACyT (Mexico), A. P. Sloan Foundation, Research Corporation, and Alexander von Humboldt Foundation.

*Also at University of California at San Diego, La Jolla, CA 92093, USA.

[1] P. Harrison and H. Quinn, SLAC Technical Report No. SLAC-R-504, 1998.
[2] Y. Grossman, Z. Ligeti, and E. Nardi, Phys. Rev. D **55**, 2768 (1997).
[3] H. E. Logan and U. Nierste, Nucl. Phys. **B586**, 39 (2000).
[4] K. Babu and C. Kolda, Phys. Rev. Lett. **84**, 228 (2000).
[5] B. Aubert *et al.* (*BABAR* Collaboration), Nucl. Instrum. Methods Phys. Res., Sect. A **479**, 1 (2002).
[6] D. Lange, Nucl. Instrum. Methods Phys. Res., Sect. A **462**, 152 (2001).
[7] S. Agostinelli *et al.* (GEANT Collaboration), Nucl. Instrum. Methods Phys. Res., Sect. A **506**, 250 (2003).
[8] The Crystal Ball function is defined to be

$$X(m) = \begin{cases} [1 + \alpha(m - m_0)/n\sigma - \alpha^2/n]^{-n} \exp[-\frac{1}{2}\alpha^2] \\ \exp[-(m - m_0)^2/2\sigma^2] \end{cases}$$

for $(m - m_0) < \sigma\alpha$ (top) and $(m - m_0) \geq \sigma\alpha$ (bottom).
[9] The ARGUS function is defined to be $A(m) = m\sqrt{1 - (m/m_c)^2}\exp\{a[1 - (m/m_c)^2]\}$.
[10] Charge conjugate states are included implicitly throughout this Letter.
[11] B. Aubert *et al.* (*BABAR* Collaboration), Phys. Rev. Lett. **92**, 071802 (2004).
[12] S. Eidelman *et al.*, Phys. Lett. B **592**, 1 (2004).
[13] P. Golonka, B. Kersevan, T. Pierzchala, E. Richter-Was, Z. Was, and M. Worek, Comput. Phys. Commun. **174**, 818 (2006).
[14] R. Barlow, Comput. Phys. Commun. **149**, 97 (2002).